

Microstructural analysis of SiC/SiC composites by X-ray tomography scans of progressive CVI matrix deposition

Y. Chen^{1a}, T.J. Marrow¹, J. Braun², C. Lorrette²

¹Department of Materials, University of Oxford, OX1 3PH, UK, ²Université Paris-Saclay, CEA, Service de Recherches Métallurgiques Appliquées, Gif-sur-Yvette, F-91191, France

^aemail of presenting author: yang.chen@materials.ox.ac.uk

Abstract. SiC/SiC composites are a candidate material for fuel cladding tubes in fission nuclear power plants. Under external mechanical loading, this material exhibits a pseudo-ductile behaviour as the macroscopic consequence of internal matrix micro-cracking. The evolution of the micro-cracks, which influence the elastic, thermal and environmental barrier properties, is strongly dependent on the composite microstructure. Image-based numerical simulations of damage evolution therefore require accurate representation of the microstructure, and can be guided by techniques such as X-ray computed tomography (XCT). To address the problem of low contrast between SiC fibres and SiC matrix, we have applied successive XCT scans to incremental matrix depositions by chemical vapour infiltration to examine the development of the SiC matrix and porosity.

Introduction

High-temperature resistance and neutron transparency are the two major advantages of SiC/SiC composites for nuclear applications. One concept for nuclear-grade SiC/SiC composites is to fabricate microstructures with relatively high porosity to encourage stable micro-cracking, thus producing higher elastic compliance and damage tolerance at the macroscopic level [1,2]. The chemical vapour infiltration (CVI) technique is used, due to its capability of controlling the final porosity with relatively high precision. The benefit of this precise control is a high reproducibility of the nonlinear material behaviour, which is an important safety requirement in nuclear applications. Although such crack-driven pseudo-ductility is highly reproducible, in order to improve material design and lifetime prediction it is crucial to understand how the composite fibrous architecture accommodates damage and deformation. Efforts have been made in this direction using in-situ surface observation [3,4] and 3D X-ray computed tomography (XCT) [5,6]. The XCT studies provide valuable 3D information on cracks and pores, but the SiC fibres and SiC matrix have never been successfully separated due to their quasi-identical X-ray attenuation coefficients. This is important as the matrix and fibres can have different responses to neutron irradiation. Observations with scanning electron microscope (SEM) have suggested that a strong inhomogeneity of matrix distribution may exist after the CVI process [7]. It is still unclear how this inhomogeneity appears in 3D, though the latter is essential for interpreting experimental observations and to build faithful numerical models. Motivated by this lack of knowledge, a procedure that uses XCT to interrogate the microstructure of SiC/SiC composites at different stages of the manufacturing process was designed.

Method

Tubes in the conventional geometry of nuclear fuel cladding were first made by filament winding of SiC fibres. Glass cylinder mandrels (diameter ~8 mm) were used as support during the filament winding process that built a fibrous wall thickness of approximately 0.6 mm. After an initial XCT scan, these filament-wound tubes were passed to the 1st CVI step to deposit a thin layer of pyrocarbon and then a thin layer of SiC matrix. Then, they were XCT scanned again using the same imaging parameters. During these two first scans, the glass cylinder mandrels were not removed in order to prevent fibres movement during transport and manipulation. A 2nd CVI step was then performed to reach the design final porosity of each tube. To facilitate image registration of the XCT scans, a small hole (1~2 mm) was drilled as a fiducial marker using diamond bit; the hole is sufficiently small so that serious damage of the fibre preform is avoided, yet large enough to be easily found even after the 2nd CVI. The XCT scans were conducted at University of Oxford using a Zeiss Xradia Versa 510 microscope (1601 projections, 60 kV, 20 s per projection). To increase the field of view (FOV), in each scan 5 tomographs were recorded at overlapping vertical positions to obtain a single tomograph using the vertical stitching algorithm of the Zeiss reconstruction software. A total FOV of 11×11×40 mm³ were achieved with voxel size of 5.5 μm.

Preliminary result

In order to facilitate the manipulation of the images, the tubular shaped composite was digitally “unwrapped” into a cuboid shape. This unwrapping procedure had been implemented and used by [8]. Zoomed-in cross-sectional slices within the cuboid (unwrapped) configuration are illustrated in Figure 1, taken from the same location in the SiC/SiC tube at different CVI stages. The features of the fibre architecture can be well recognised. This indicates that the CVI process had no significant effect on the arrangement of fibres in terms of location and shape. This makes it possible to quantify the distributions of elementary phases (fibres, matrix and pores) at the local scale with a relatively good precision.

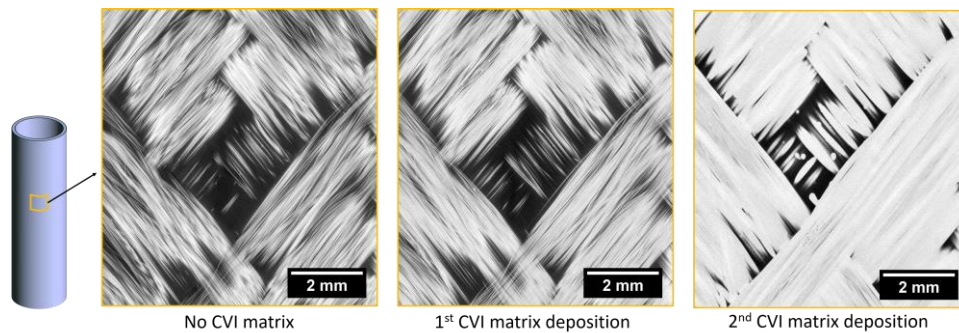


Figure 1. Zoomed-in region in three XCT images of the same location in the SiC/SiC tube at different CVI steps. The fibres and matrix are light.

The successive images were manually registered. The results on a larger region are illustrated in Figure 2, which considers the change between the 1st and 2nd CVI steps. In the comparison image (colour + grey), magenta highlights the SiC pixels that are not found in the upper image (1st CVI) but are found in the middle image (2nd CVI); whereas green highlights those found in the upper image but not found in the middle image. Very few green pixels can be seen from the comparison image, since SiC introduced in the first CVI obviously did not disappear after the final CVI. The magenta pixels are mostly located at the inner and outer surfaces, as well as around the macropores, which is consistent with the expectation for the CVI deposition process.

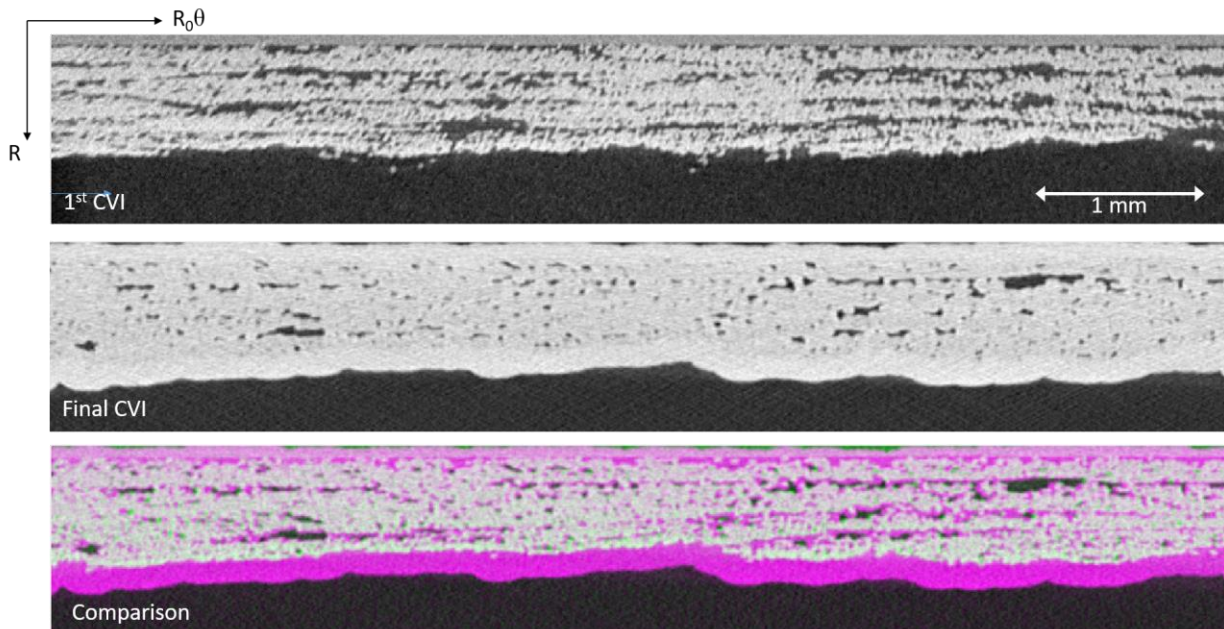


Figure 2. Result of image registration – comparison between the successive images at 1st and 2nd CVI.

Conclusion

This work demonstrated the use of XCT to progressively study the evolution of the phase distribution in SiC/SiC composites at incremental CVI steps. The fibre architecture was very stable throughout the CVI process, i.e. no obvious fibre movement even at a local scale ($\sim 10 \mu\text{m}$). Image registration allowed the matrix distribution in the 3D microstructure to be examined. The quantitative analysis in progress will allow high-fidelity simulations of CVI processes SiC/SiC composites that consider the distribution and properties of matrix and fibres that may respond differently to environmental factors such as the neutron irradiation dose.

References

- [1] C. Mingazzini et al., 2018 IEEE International Conference on Environment and Electrical Engineering and 2018 IEEE Industrial and Commercial Power Systems Europe (EEEIC / I&CPS Europe), Palermo, Italy, 2018, pp. 1-6, doi: 10.1109/EEEIC.2018.8494444.
- [2] Braun, J., Sauder, C., Lamon, J., & Balbaud-Célérier, F. (2019). *Comp. Part A*, 123, 170-179.
- [3] Bernachy-Barbe, F., Gélébart, L., Bornert, M., Crépin, J., & Sauder, C. (2015). *Comp. Part A*, 68, 101-109.
- [4] Tracy, J. M. (2014). *Multi-scale Investigation of Damage Mechanisms in SiC/SiC Ceramic Matrix Composites* (Doctoral dissertation).
- [5] Saucedo-Mora, L., Lowe, T., Zhao, S., Lee, P. D., Mummery, P. M., & Marrow, T. J. (2016). *Journal of Nuclear Materials*, 481, 13-23.
- [6] Chen, Y., Gelebart, L., Chateau, C., Bornert, M., King, A., Sauder, C., & Aïmedieu, P. (2020). *Journal of the European Ceramic Society*, 40(13), 4403-4418.
- [7] Chateau, C., Gélébart, L., Bornert, M., & Crépin, J. (2015). *International Journal of Solids and Structures*, 58, 322-334.
- [8] Chen, Y., Gélébart, L., Chateau, C., Bornert, M., King, A., Aïmedieu, P., & Sauder, C. (2020). *Experimental Mechanics*, 60(3), 409-424.